Micromachined Horn Antenna Operating at 75 GHz

Tomasz M. Grzegorczyk[1], Jean-François Zürcher[1], Philippe Renaud[2] and Juan R. Mosig [1]

[1] Laboratoire d'Electromagnétisme et d'Acoustique (LEMA) Ecole Polytechnique Fédérale de Lausanne (EPFL), 1015 Lausanne, Switzerland, (Tomasz.Grzegorczyk@epfl.ch);
[2] Institut de Microsystèmes (IMS), Ecole Polytechnique Fédérale de Lausanne (EPFL), 1015 Lausanne, Switzerland.

***Abstract*—We propose in this paper an integrated cavity-backed horn antenna, generalizing the well-known SSFIP (Strip-Slot-Foam-Inverted Patch) design, operating at 75 GHz. The antenna was optimized using a full-wave software and realized using micromachining technologies. The proposed structure can be used for high radiation efficiency antennas and arrays in the millimeter-wave band, since surface waves are inherently suppressed by the use of a metallic horn and a cavity configuration.**

I. Introduction

The rapid growth of telecommunication technologies has been an opportunity for microstrip antennas to prove all there capabilities and versatility. Still nowadays, with the ever increasing operating frequencies, their simplicity, adaptability and low fabrication costs represent tremendous advantages, which keep innovative microstrip antenna designs in the scope of research.

Concerned about the ever reduced size of antennas required for industrial applications, we propose in this paper an SSFIP (Strip-Slot-Foam-Inverted Patch) horn antenna operating at 75 GHz, for which a generic layout is shown in fig. 1. Due to the complexity of the structure, two main challenges had to be faced. First, a theoretical study had to be undertaken (see section II), aiming at an accurate prediction of the input impedance of the device. This means that all the complex elements (the horn, the cavity and the semi-infinite substrate) had to be accurately modeled and Maxwell's equations solved in the corresponding environments. Second, the technological approach had to be revised since the classical techniques used in the C-band failed to provide reliable results. Hence, we have adopted a similar approach to the one presented in [1], [2], namely the use of micromachining technologies already successfully applied in various domains [3], [4]. More details are given in section III, where some steps of the antenna fabrication are presented.

II. Theoretical formulation of the problem

A possible way to solve Maxwell's equations in the different environments of the antenna shown in fig. 1 is to use the integral equation technique [5] with the appropriate Green's functions. The latter are of two kinds:

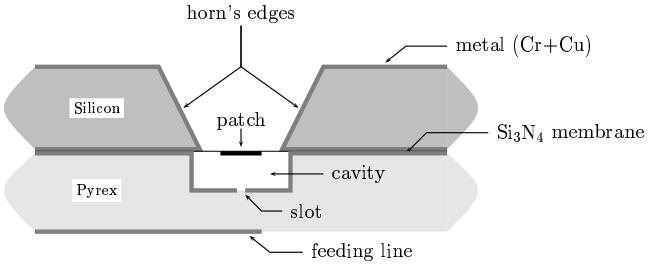

Fig. 1.: General layout of the integrated SSFIP-horn antenna. The upper part is realized in a silicon wafer whereas the lower part in a pyrex wafer. The darker grey lines represent the metal (chrome and copper) deposited on the wafers.

1. *Boxed*, for the modeling of the cavity [6] and the horn (which is approximated by a succession of straight waveguide discontinuities [7], yielding good results not only for real corrugated horns but also for smooth ones). These Green's functions are expressed as an infinite sum of modes weighted by coefficients taking into account the longitudinal dimensions of the medium [8]. Written in this way, they are particularly well-adapted to the study of layered media in shielded environments.

2. *Laterally infinite*, for the modeling of the substrate above the feeding line. This type of Green's functions has already been widely studied in the frame of multilayered media [9]–[12] and is thus already well mastered. The theoretical results presented in this paper have been obtain using the spectral closed-form expressions given in [12], and the spatial counterparts have been obtained through Sommerfeld integrals [13], for which judicious numerical algorithms have been implemented in order to reduce the computation time [14].

These Green's functions have been further used in a mixed potential integral equation (MPIE) formalism, which has been solved by a Galerkin version of the method of moments (MoM) [15]. It should be mentioned that working with the MPIE is a purely numerical choice, since the kernel of the Green's functions for the potentials presents a milder singularity than that for the fields (r^{-1} instead of r^{-3}), rendering the self-interactions in the MoM matrix numerically computable (the singularity having the additional advantage of being removable).

All these theoretical considerations have been implemented in a general numerical code providing an accurate tool for the simulation of antennas close to the generic one presented in fig. 1. Thus, an optimization of the original device (concerning both the dimensions of the various elements and the materials used) has been performed, leading to the following results:

– membrane: $2300\mu m \times 2300\mu m$;

– patch: $1600\mu m \times 1600\mu m$;

– cavity: $3200\mu m \times 3200\mu m$ etched in pyrex ($\varepsilon_r \simeq 4.4$) over a depth of about $200\mu m$;

– slot: $980\mu m \times 80\mu m$;

– feeding line: adaptive width from $1290\mu m$ down to $672\mu m$ (in order to keep a constant 50Ω characteristic impedance).

It is important to notice that the cavity below the radiating patch increases the overall efficiency of the antenna by suppressing the surface waves, which propagate in the substrate and which are in general responsible for a non negligible loss of power. However, as it can be seen in fig. 1, this is only partially achieved since these waves may still propagate between the feeding line and the slot. To justify that this is not a hindrance in our case, we should recall the theory of complex functions and various considerations about the complex plane topology. Since this is already beyond the scope of this paper, we shall not enter into details here but refer the reader to [16], [17]. We can nevertheless mention that the laterally propagating waves correspond to the singular points (saddle point, branch point and poles) of the spectral Green's functions that, depending on their location in the complex plane, can excite either space waves (saddle point), surface waves (for the poles located in the proper Riemann sheet) or leaky waves (if they are in the improper Riemann sheet). Our overall goal is thus to have as few singular points as possible, which can be achieved for example by lowering the dielectric constant of the substrate. The pyrex ($\varepsilon_r \simeq 4.4$) has been found to be a good compromise between this requirement and the technological ones (rigidity, ease of manufacturing and cost).

III. Technological realization at 75 GHz

The technological realization of the antenna has been done in two major steps, each performed on a separate wafer (see fig. 1). The first one was a $<100>$ low doped ($< 10^{19}$) silicon wafer on which a $1\mu m$-thick low-stress Si_3N_4 membrane has been evaporated. The sole purpose of the silicon in our case is to be a mechanical support for the membrane and the radiating element (the patch), an exception being the horn which has been etched along the natural planes of the crystal (a $< 100 >$ orientation giving an apex angle of 70.6°).

The second one (pyrex) supported the feeding elements represented by the microstrip line on the back, the coupling slot and the cavity. The proper optimization of these three parameters being of the foremost importance for the matching of the antenna, the related technological steps should be performed with great care.

The overall technological process applied to the two wafers has been the following:

1. *Silicon wafer* (thickness $\simeq 380\mu m$). A general preparation has been done (HNO_3 and BHF cleaning), followed by the deposition of metals. The latter has been performed in two steps: first an evaporation of chrome for a better adherence and of copper for a first contact layer, second a galvanization of copper to reach a thickness of about 5 μm, which is large enough compared to the skin-depth at these frequencies. The next step followed a classical photolithographic process in order to pattern the front and back side of the wafer (the Si_3N_4 membrane being removed by plasma etching). After another metallization run, the silicon has finally been etched in a KOH bath, revealing the $1\mu m$-thick membrane supporting the patch.

2. *Pyrex wafer* (thickness $\simeq 500\mu m$). In view of a quite severe chemical attack to etch the cavity, the process of the pyrex wafer started by the deposition of a double mask: a layer of chrome (cold sputtering) over which a negative SC450 photoresist has been spun. Once the photolithographic process accomplished, the attack has been done for about half an hour in a 50% HF solution heated at 30°c to reach an etch depth of 200μm, and the remaining negative photoresist has been removed in Piranah solution (five minutes bath). The final steps followed a classical photolithographic procedure in order to deposit the metals (chrome and copper) on both sides of the wafer and pattern the different elements (the slot on the front side and the feeding line on the back). A top view of the final chip is depicted in fig. 2(a) where an additional canal for the air evacuation can be seen, the latter maintaining a constant pressure inside the cavity.

Once both steps have been accomplished, the final task was to connect the two wafers one on top of the other. The perfect alignment was ensured by the various marks printed on their surfaces, leading to the final result shown in fig. 2(b).

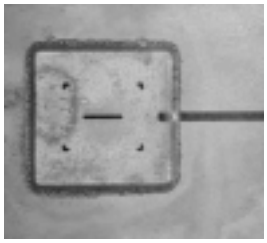

(a) Top view of the pyrex wafer (slot, cavity, alignment marks and evacuation canal).

(b) View of the silicon wafer stacked on the pyrex one.

Fig. 2.: Photographs of the antenna: (a) pyrex wafer alone, (b) silicon wafer stacked on top of the pyrex one.

IV. Results and Conclusions

The antenna has been realized following the steps described in section III and matching the optimized dimensions given in section II, which correspond to an operating frequency of 75 GHz. The input impedance was measured on a HP 8510XF network analyzer in the [70-80] GHz frequency range, and the comparison between the theoretical predictions and the measurements is shown in fig. 3. As it can be seen, there is a small shift of about 4% in the operating frequency. This can be due to several reasons, involving both the lack of accuracy of some technological steps and the difficulty to perform electromagnetic measurements at these frequencies. For instance, we can mention:

– the imprecise knowledge of the pyrex thickness (the reported values are 500μm $\pm 50\mu$m),

– the difficulty to ensure a homogeneous cavity depth,

– the expected high losses at these frequencies,

– the general ripples inherent to wave reflections difficult to control at millimeter-wave frequencies.

However, despite all these uncertainties, the agreement is satisfactory in both the resonant frequency and the level of matching. Consequently, we have shown that the technology involved in the fabrication of this type of antenna is now mature and, combined to an accurate electromagnetic analysis software, can lead to reliable designs and small development time.

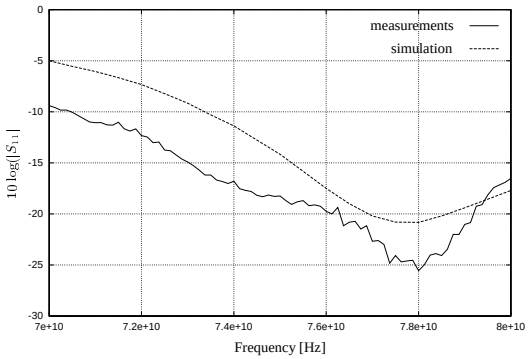

Fig. 3.: Comparison between measurements and simulation of the integrated horn antenna of fig. 1.

REFERENCES

[1] W. Y. Ali-Ahmad, W. L. Bishop, T. W. Crowe, and G. M. Rebeiz, "An 86-106 ghz quasi-integrated low noise shottky receiver," *IEEE Transactions on Microwave Theory and Techniques*, vol. 41, pp. 558–564, April 1993.

[2] G. P. Gauthier, J.-P. Raskin, L. P. Katehi, and G. M. Rebeiz, "A 94-GHz aperture-coupled micromachined microstrip antenna," *IEEE Transactions on Antennas and Propagation*, vol. 47, pp. 1761–1766, December 1999.

[3] C.-Y. Chi and G. M. Rebeiz, "Planar microwave and millimeter-wave lumped elements and coupled-line filters using micro-machining techniques," *IEEE Transactions on Microwave Theory and Techniques*, vol. 43, pp. 730–738, April 1995.

[4] I. Papapolymerou, R. F. Drayton, and L. P. Katehi, "Micromachined patch antennas," *IEEE Transactions on Antennas and Propagation*, vol. 46, pp. 275–283, February 1998.

[5] J. R. Mosig, "Arbitrarily shaped microstrip structures and their analysis with a mixed potential integral equation," *IEEE Transactions on Microwave Theory and Techniques*, vol. 36, pp. 314–323, February 1988.

[6] A. A. Melcón and J. R. Mosig, "Strip, slot, air, inverted patch (SSAIP): A cavity backed alternative to broadband communication antennas," *Radio Science*, vol. 33, pp. 1525–1542, November-December 1998.

[7] T. M. Grzegorczyk, J.-F. Zürcher, and A. K. Skrivervik, "Analysis of a horn antenna by the integral equation method," in *JINA conference*, (Nice, France), pp. 92–95, 17-19 November 1998.

[8] N. Marcuvitz, *Waveguide Handbook.* M.I.T. Radiation Laboratory Series, Boston Technical Publishers, Inc., 1964.

[9] N. Kinayman and M. I. Aksun, "Efficient use of closed-form Green's functions for the analysis of planar geometries with vertical connections," *IEEE Transactions on Microwave Theory and Techniques*, vol. 45, pp. 593–603, May 1997.

[10] Y. L. Chow, N. Hojjat, S. Safavi-Naeini, and R. Faraji-Dana, "Spectral Green's functions for multilayer media in a convenient computational form," *IEE Proceedings on*

Microwave Antennas and Propagation, vol. 145, pp. 85–91, February 1998.

[11] K. A. Michalski and J. R. Mosig, "Multilayered media Green's functions in integral equation formulations," *IEEE Transactions on Antennas and Propagation*, vol. 45, pp. 508–519, March 1997.

[12] T. M. Grzegorczyk and J. R. Mosig, "Full-wave analysis of antennas containing horizontal and vertical metalizations embedded in multilayered media," *IEEE Transactions on Antennas and Propagation*, 2000. Submitted for publication.

[13] A. Sommerfeld, *Partial Differential Equations in Physics*. Academic Press, 1964.

[14] J. R. Mosig and F. Gardiol, "Analytical and numerical techniques in the Green's function treatment of microstrip antennas and scatterers," *IEE Proceedings (part H)*, vol. 130, pp. 175–182, March 1983.

[15] R. F. Harrington, *Field Computation by Moment Method*. IEEE Press, 1993. ISBN 0-7803-1014-4.

[16] L. Felsen and N. Marcuvitz, *Radiation and Scattering of Waves*. Electrical Engineering Series, Prentice Hall, 1973. ISBN 0-7803-1088-8.

[17] J. A. Kong, *Theory of Electromagnetic Waves*. John Wiley & Sons, 1975. ISBN 0-471-50190-5.